**Network specific change in white matter integrity in mesial temporal lobe**

**epilepsy.**

Hisaji Imamura[a] [1], Riki Matsumoto[b], Shigetoshi Takaya[c, f, g], Tomokazu Nakagawa[a],

Akihiro Shimotake[a], Takayuki Kikuchi[d], Nobukatsu Sawamoto[a], Takeharu Kunieda[d],

Nobuhiro Mikuni[d, e], Susumu Miyamoto[d], Hidenao Fukuyama[c],

Ryosuke Takahashi[a], Akio Ikeda[b]


a.  *Department of Neurology, Kyoto University Graduate School of Medicine, 54*

    *Shogoin Kawahara-cho, Sakyo-ku, Kyoto, 606-8507, Japan*

b.  *Department of Epilepsy, Movement Disorders and Physiology, Kyoto University*

    *Graduate School of Medicine, 54 Shogoin Kawahara-cho, Sakyo-ku, Kyoto,*

    *606-8507, Japan*

c.  *Human Brain Research Center, Kyoto University, 54 Shogoin Kawahara-cho,*

    *Sakyo-ku, Kyoto, 606-8507, Japan*

d.  *Department of Neurosurgery, Kyoto University Graduate School of Medicine, 54*

    *Shogoin Kawahara-cho, Sakyo-ku, Kyoto, 606-8507, Japan*

e.  *Department of Neurosurgery, Sapporo Medical University, S1 W17, Chuo-ku,*

*Sapporo, 060-8556, Japan*

f.  *Radioisotope Research Center, Kyoto University, Kyoto, 606-8315, Japan*

g.  *A. Martinos Center for Biomedical Imaging, Massachusetts General Hospital,*

    *Harvard Medical School, MA 02129, USA*

*Present address*

*1. Hisaji Imamura, Department of Neurology, Fukui Red Cross Hospital, 4 Tsukimi,*

*Fukui, 918-8501, Japan*


*E-mail*

*Hisaji Imamura, imamurah@kuhp.kyoto-u.ac.jp*

*Riki Matsumoto, matsumot@kuhp.kyoto-u.ac.jp*

*Shigetoshi Takaya, shig.t@kuhp.kyoto-u.ac.jp*

*Tomokazu Nakagawa, tnakaga@kuhp.kyoto-u.ac.jp*

*Akihiro Shimotake, smtk@kuhp.kyoto-u.ac.jp*

*Takayuki Kikuchi, tkik@kuhp.kyoto-u.ac.jp*

*Nobukatsu Sawamoto, sawa@kuhp.kyoto-u.ac.jp*

*Takeharu Kunieda, kuny@kuhp.kyoto-u.ac.jp*

*Nobuhiro Mikuni, mikunin@sapmed.ac.jp*

*Susumu Miyamoto, miy@kuhp.kyoto-u.ac.jp*

*Hidenao Fukuyama, fukuyama@kuhp.kyoto-u.ac.jp*

*Ryosuke Takahashi, ryosuket@kuhp.kyoto-u.ac.jp*

*Akio Ikeda, akio@kuhp.kyoto-u.ac.jp*

*Corresponding to: Riki Matsumoto & Akio Ikeda, Kyoto University Graduate School*

*of Medicine, 54 Shogoin Kawahara-cho, Sakyo-ku, Kyoto, 606-8507, Japan*

Tel & fax:        +81-75-751-3772 & +81-75-751-9416

E-mail:  matsumot@kuhp.kyoto-u.ac.jp (RM), akio@kuhp.kyoto-u.ac.jp (AI)

**Title:** 83 characters

Text: 20 pages, 4192 words

5 figures, 1 table, 1 supplementary figure

**Summary**

**Objectives:** To identify the specific change of white matter integrity that occurs in the

brain network related to epileptic activity in patients with mesial temporal lobe epilepsy

(MTLE).

**Methods:** We recruited 18 patients with MTLE and 18 healthy subjects. In MTLE patients,

the remote functional-deficit zone was delineated using fluorodeoxyglucose positron

emission tomography as an extratemporal region showing glucose hypometabolism. Using

diffusion magnetic resonance imaging tractography, we defined a seizure propagation tract

(PT) as a white matter pathway that connects the focus with a remote functional deficit

zone. We also used the corticospinal tract (CST) and inferior longitudinal fasciculus (ILF)

as control tracts in the hemisphere ipsilateral to the focus. Fractional anisotropy (FA),

mean diffusivity (MD), and volume of the tracts were compared among PT, CST, and ILF.

**Results:** Tractographic analysis identified the uncinate fasciculus, arcuate fasciculus, and

fornix as PTs. A decrease in FA was found in MTLE patients compared with healthy

subjects in all tracts, but PTs showed a more significant decrease in FA than did the two

control tracts. Although the change in MD was also found in MTLE patients compared

with healthy controls, a tract-specific change was not observed. Although white-matter

damage was observed in all candidate tracts examined, the integrity of white matter was

most significantly decreased in PTs in MTLE.

**Conclusion:** The change in white matter integrity occurs specifically in the pathways that

connect the focus and remote functional deficit zones in patients with MTLE, i.e., the

pathways that are assume to be associated with seizure propagation.

1 **Introduction**

1.1    In patients with mesial temporal lobe epilepsy (MTLE), glucose hypometabolism often extends beyond the temporal lobe. Among them, glucose hypometabolism in the prefrontal cortex is associated with cognitive changes (Jokeit et al., 1997; Takaya et al., 2006), suggesting that functional deficit zones exist in the remote cortical regions (Rosenow and Luders, 2001).

1.2    Glucose hypometabolism in the remote cortical regions from the epileptic focus reflects the preferential networks involved by ictal discharges and is also associated with seizure frequency (Chassoux et al., 2004; Takaya et al., 2006). In addition, after the epileptogenic lesion in the mesial temporal lobe is removed, the remote areas that supposedly receive projections from the affected area show improved glucose metabolism (Dupont et al., 2001; Spanaki et al., 2000; Takaya et al., 2009). These lines of evidence suggest that the functional deficit zones in remote cortical regions are most likely the result of the frequent propagation of epileptic activity from the epileptic focus through a white matter pathway.

1.3    Previous studies using voxel-wise whole brain analysis of white matter integrity such as tract-based spatial statistics (TBSS) have shown that the change in white matter integrity occurs throughout the brain in patients with MTLE (Focke et al., 2008;

Schoene-Bake et al., 2009; Yogarajah et al., 2010). One possible reason is that inherent

pre-existing abnormalities due to genetic factors or developmental abnormalities might

exist in the whole brain in patients with MTLE (Velisek and Moshe, Epilepsia 2003; Love,

Lancet Neurol 2005). However, whether there is any pathway that is specifically impaired

compared with other white matter pathways in patients with MTLE remains unclear. Given

that the epileptic activity arising from the focus is assumed to generate the functional

deficit zone in remote cortical regions through white matter pathways as mentioned above,

we would hypothesize that epileptic activity specifically impairs these pathways.

1.4      In this study, we first delineated the white matter pathways that connect the focus

and the remote functional deficit zones in MTLE patients by combining FDG-PET and

diffusion MRI tractography. We traced these specific white matter pathways into the

cortices that showed glucose hypometabolism in FDG-PET by adopting probabilistic

diffusion tractography that can trace beyond region of high uncertainty into the grey matter

or across the crossing fibers (Behrens et al., 2007). Then we evaluated the change in white

matter integrity of these pathways using tractography-based regions of interest (ROI)

method. The advantage of this method is that it allows the cross-subject comparison of

white matter integrity along the given tracts without requiring cross-subject registration

(Smith et al., 2013). We expected to see that the pathway that connects the focus and the

remote functional deficit zones is affected much more than other white matter pathways.

Our findings may provide insight into the wide range of functional network impairment in patients with localization-related epilepsy.

## 2 Methods

### 2.1 Subjects

2.1.1    We recruited 18 right-handed patients with medically intractable MTLE (10 with left MTLE and 8 with right; mean age, 30.7 years; ranging, 19–45 years; 8 men, 10 women). All patients underwent presurgical evaluation between 2007 and 2010 at the Kyoto University Hospital. These patients were diagnosed as MTLE on the basis of seizure semiology, electroencephalography (EEG), video EEG monitoring, and neuroimaging data. We detected hippocampal atrophy or sclerosis in all 18 MTLE patients by means of 3-tesla MRI. Patients with additional MRI anomalies outside the mesial temporal lobe were excluded from this study. Eight patients underwent surgery. Ten patients are on a waiting list for surgery. The details of the patients' demographic data are shown in table 1. We also analyzed 18 age-matched right-handed healthy control subjects (mean age, 31.3 years; ranging, 18–47 years; 10 men, 8 women).

**2.2 Standard Protocol Approvals, Registrations, and Patient Consents.**

2.2.1    This study was approved by the Ethics Committee of Kyoto University Graduate

School of Medicine (approval# E-430), and written informed consent was obtained from

all patients and healthy volunteers.

**2.3 FDG-PET data analysis**

**2.3.1**    The FDG-PET scans were performed using a PET scanner (Advance, General

Electric Medical System, Milwaukee, WI, USA). [18F]-FDG at 370 MBq (10mCi) was

injected intravenously into subjects who had been fasting for at least four hours. Then, 40

minutes after the administration of the radiotracer, 35 slices of brain-emission images were

acquired over a 20-min period. The subjects were studied in an awake, resting state, with

their eyes closed and ears unplugged in a dimly lit environment. Although EEG was not

recorded during FDG-PET study, it was unlikely an ictal study because no abnormal

behaviors were observed, and because patients did not report any subjective manifestations

of seizure during the examination. Emission images were reconstructed into a 128 x 128

matrix image with a pixel size of 1.95 x 1.95 mm$^2$ and slice thickness of 4.25 mm. All

reconstructed images were corrected for attenuation using $^{68}$Ge-$^{68}$Ga transmission scans

performed before the actual scan. The FDG-PET images from the patients with right

MTLE were flipped so that the epileptic focus was on the left side in all images. Images

from the same number of healthy volunteers were also flipped. Voxelwise analysis of the

FDG-PET images was performed using Statistical Parametric Mapping 8 (SPM8). The

FDG-PET images were coregistered with the anatomical three-dimensional (3D) MRI

images of each person by means of the mutual information algorithm implemented in

SPM8. The flipped FDG-PET images of the patients with right MTLE and the same

number of healthy volunteers were coregistered with the flipped MRI images. The

coregistered FDG-PET images were then spatially normalized to fit an in-house FDG-PET

template using affine and nonlinear warping. The spatially normalized images were

smoothed using an isotropic Gaussian kernel with 16-mm full width at half maximum

(FWHM) to increase the signal-to-noise ratio and to account for normal interindividual

macroanatomical variation. To eliminate the effects of global neuronal activity, each voxel

count was normalized to the total count of the whole brain using proportional scaling.

2.3.2     A two-sample $t$ test was used for the voxelwise group comparison of the

FDG-PET images between patients and healthy volunteers. Adjustment for gender as a

confounder was performed by using it as a nuisance variable. We analyzed the brain

regions showing a decrease in glucose metabolism at the height threshold ($p = 0.001$;

uncorrected for multiple comparison) and an extent threshold of 300 voxels. Thus, a

hypometabolic region, i.e., a functional deficit zone was identified in the MTLE group in

the Montreal Neurological Institute (MNI) standard space (figure 1A). The hypometabolic

region was observed within the following two regions: 1) the temporal lobe ipsilateral to

the focus, i.e., the anterior lateral and basal temporal areas, which included both the

hippocampus and parahippocampus that were thought to be the epileptic focus and 2) the

ipsilateral extratemporal area, i.e., the ventrolateral prefrontal area.

## 2.4 MRI data acquisition

2.4.1     Magnetic resonance images were acquired on a 3-T Siemens Trio scanner.

Diffusion weighted image (DWI), dual-gradient field map, and three-dimensional (3D)

anatomical image were acquired using a 3.0 Tesla MRI scanner (Trio, Siemens, Erlangen,

Germany) with an eight-channel phased-array head coil. DWI was acquired using

single-shot spin-echo echo-planar sequence. The scanning parameters as follows: echo

time (TE) = 96 ms; repetition time (TR) = 10,500 ms; flip angle (FA) = 90; field of view

(FOV) = 192 x 192 mm2; slices = 70; voxel size = $2 \times 2 \times 2$ mm. The diffusion weighting

was isotropically distributed along 81 directions using a b value of 1,500 s/mm2. Nine

volumes of no diffusion weighting (b = 0 s/mm2 ) were also acquired at points throughout

the acquisition. Dual-gradient field map in an axial orientation was obtained for the b0

unwarping of DWI using the following parameters: TR = 511 ms; TE1/TE2 = 5.19/7.65

ms; FA = 60°; FOV = 192 × 192 mm; slices = 46; voxel size = 3 × 3 × 3 mm. The scanning

parameters of T1-weighted three-dimensional anatomical images [Magnetization Prepared

Rapid Gradient Echo, (MPRAGE)] were as follows: TE = 4.38 ms; TR = 2,000 ms;

176×292 matrix; FOV = 176 mm×292 mm2; slice of 1.0 mm thickness. The details of

acquisition of diffusion-weighted images (DWI), a dual-gradient field map, 3D anatomical

images, and postprocessing of the DWI data (Diffusion tensor imaging and probabilistic

diffusion tractography) have been reported elsewhere (Oguri et al., 2013; Yamao et al.,

2014).

**2.5 Tractography-based assessment of white matter integrity along the tracts**

2.5.1     We herein defined a putative propagation tract (PT) of epileptic activity as a white

matter tract that connects the epileptic focus and a remote functional deficit zone. As

control tracts, we selected the inferior longitudinal fasciculus (ILF) and the corticospinal

tract (CST). The ILF was chosen because both the PT and the ILF usually originate from

the anterior and basal temporal areas (Catani et al., 2003), whereas the target cortical

region is different (the frontal functional deficit zone versus the occipital lobe). The CST

was selected as a tract that was away from the epileptic focus in the temporal lobe. Both

control tracts were reported to show good reproducibility during identification of tracts

using diffusion tractography (Wakana et al., 2007).

2.5.2    In order to identify the PT, the seed region of interest (ROI) was placed in the

hypometabolic temporal area that comprised the epileptic focus. This is partly because of a

technical limitation: it is difficult to perform diffusion tractography directly on the

hippocampus because diffusion-weighted signals are often distorted there because of air

susceptibility artifacts. Moreover, atrophy was present in the MTLE group. From the

standpoint of the "epileptogenic zone"(Rosenow and Luders, 2001), it is also difficult to

confine the focus to the hippocampus alone. The epileptogenic zone in MTLE is not

always restricted to the hippocampus but occasionally is present in the temporal pole and

the basal part (Coste et al., 2002; Moran et al., 2001). Furthermore, according to other

FDG-PET studies, the hypometabolic temporal area surrounding the hippocampus is

related to generation of ictal discharge and spread pathways (Chassoux et al., 2004).

According to these pieces of evidence, in the present tractography study, we decided to

place the seed ROI in the hypometabolic temporal region. The target ROI of PT was placed

in the frontal hypometabolic region that represented the extratemporal functional deficit

zone. To divide the hypometabolic region into the temporal and frontal subregions, we

manually set a 3-mm-thick boundary between the two subregions at the border of the two

lobes (3 mm thick; a white mask in figure 1B). These ROIs were set up in the MNI

standard space. For the left-MTLE patients and the same number of randomly assigned

healthy volunteers, these ROIs were transferred to the T1 anatomical space in each subject

using the inverted transformation matrices of spatial normalization. For the right-MTLE

patients and the rest of healthy volunteers, we flipped the ROIs in the MNI space so that

they were located in the right hemisphere, and then we transferred them to the T1

anatomical space in each individual brain.

2.5.3    In each brain, we segmented the gray matter of the seed and target ROIs using

FMRIB's Automated Segmentation Tool of the FSL software (fsl.fmrib.ox.ac.uk). These

segmented, cortical portions of the seed and target ROIs served as the seed and target

masks, respectively. To exclude erroneous pathways such as the tracts going into the

contralateral hemisphere, exclusion masks were placed on the midline sagittal plane and

the boundary between the two hypometabolic subregions (white masks in figure 1B). In

the two control tracts (CST and ILF), the seed and target masks were set up according to

the methods reported by Wakana[12] with modifications (details in the appendix). The seed

mask for inferior longitudinal fasciculus (ILF) was set at the same seed mask as used for

tracing PT, namely, the segmented temporal hypometabolic region. The target ROI was set

in the ipsilateral occipital lobe defined by the MNI atlas implemented in FSLView software.

This target ROI was transferred onto T1 anatomical space in each subject using the

inverted transformation matrices of spatial normalization. On a coronal directional

color-coded map, an additional waypoint mask was placed in the coronal plane passing

through the caudal end of the splenium of the corpus callosum. The tracts that were

situated lateral or inferior to the lateral ventricle and running in the anterior-posterior

direction were selected. The exclusion mask was set on a midline sagittal plane.

2.5.4    Regarding Cortico-Spinal-Tract (CST), the seed mask was manually set in the

cerebral peduncle ipsilateral to the focus by using the axial directional color-coded map in

each subject. The target mask was set in the ipsilateral precentral gyrus of Harvard Oxford

Atlas (www.cma.mgh.harvard.edu). The exclusion mask was set at a midline sagittal plane.

2.5.5    These target and exclusion masks were constructed in the MNI standard space,

and then transformed onto each subject's brain (MPRAGE) using the inversion

transformation matrices of spatial normalization. Those made in the directional

color-coded map in each subject's brain were also linearly coregistered onto each subject's

MPRAGE. Probtracx function of FDT was performed using these masks in MPRAGE

space.

2.5.6    Probabilistic diffusion tractography was performed for the PT and control tracts

(ILF and CST) with the aforementioned seed, target, and exclusion masks using FMRIB's

Diffusion Toolbox (FDT) of the FSL software. Probability density functions were

calculated by drawing 5,000 samples from each voxel in the seed mask. The connectivity

value was the number of samples that passed through a voxel; this number was

automatically calculated by the probtrackx function of FDT. In contrast to deterministic

streamlining tractography, we needed a certain threshold value to extract significant

tractography findings. Because no gold standard exists for the selection of the threshold,

we traced these three tracts using thresholds 0.1%, 1%, 5%, 10%, and 20% of the

maximum connectivity value calculated separately for each tract. We then calculated mean

fractional anisotropy (FA), mean diffusivity (MD), and volume of the tracts at each

threshold. Because the seed masks of PT and ILF were identical in the temporal lobe, we

masked out the tracts within the temporal hypometabolic region (both the gray- and white

matter) for measurement of FA and MD of the PT and ILF.

2.5.7    FA, MD, and volume of the tracts were subjected to repeated-measures analysis of

variance (ANOVA), with the tract (PT versus ILF versus CST) as a within-subject factor,

and the group (MTLE patients versus healthy volunteers) as a between-subject factor. If

there was a tract-by-group interaction among the three tracts, we performed *post hoc*

analysis of all three pairs (PT versus CST, PT versus ILF, and CST versus ILF). Statistical

significance was set at p < 0.05. We used the SPSS 15.0J software for statistical

calculations.

## 2.6    Voxel-wise whole brain assessment of white matter integrity

2.6.1    We also assessed white matter integrity using TBSS to see the change

that occurs throughout the whole brain in MTLE patients that has shown in previous

studies (Focke et al., 2008; Schoene-Bake et al., 2009; Yogarajah et al., 2010). In brief,

TBSS projects all subjects' FA data onto a mean FA tract skeleton, before

applying voxelwise cross-subject statistics. Both control minus patient and

patient minus control contrasts were tested, with 5,000 permutations. Multiple

comparisons were corrected using a threshold-free cluster enhancement

(TFCE) (Smith et al. 2009). Voxelwise statistical inference was made on these

output images, and significance level was set at p<0.01, corrected for

family-wise error rate.

## 3 Results

## 3.1 The putative propagation tract

3.1.1    It was traced from the temporal to the frontal functional deficit zone at several

thresholds (0.1%, 1%, 5%, 10%, and 20%). Because of the "probabilistic" nature of the

tractography, as the threshold increased, the traced tracts changed from a widespread

distribution to more restricted or focused one (figure 2). At the threshold 0.1%, too many

tracts were uncovered to extract the core PT. At the 1% threshold, three pathways were

detected. The first pathway ran through the uncinate fasciculus (UF) toward the prefrontal

cortex. The second pathway ran through the long segment of the arcuate fasciculus (AF).

The third pathway first ran through the fornix to the thalamus and ended in the prefrontal

cortex (figure 2). When the threshold was $\geq 5\%$, UF and AF became the predominant

pathways among these tracts. At the 20% threshold, only UF remained significant among

the three pathways. The seed mask encompassed the gray matter of the whole temporal

hypometabolic region for both PT and ILF, but the actual seed areas of the UF and ILF

overlapped and were confined to the anterior part of the parahippocampal and fusiform

gyri (figure 5).

## 3.2 Comparison of white matter integrity in the propagation tract and control tracts

3.2.1    The FA values of PT ($FA_{PT}$), ILF ($FA_{ILF}$), and CST ($FA_{CST}$) were compared

between the MTLE and healthy control groups. All three tracts showed decreased FA in MTLE patients. Repeated-measures ANOVA demonstrated a significant interaction between the tract (PT, IFL, or CST) and the group (patients versus healthy subjects) for all the thresholds except 0.1%: at the thresholds 1% ($p = 0.034$; $F = 3.752$), 5% ($p = 0.013$; $F = 4.927$), 10% ($p = 0.010$; $F = 5.358$), and 20% ($p = 0.022$; $F = 4.281$). Repeated-measures ANOVA also demonstrated a significant effect of the tract; the FA values were different between the three tracts (figure 3A). In pairwise analysis, significant tract-by-group interactions were observed between the PT and ILF at the thresholds 5% ($p = 0.009$; $F = 7.625$), 10% ($p = 0.003$; $F = 10.5$), and 20% ($p = 0.007$; $F = 8.3$) and between the PT and CST at the thresholds 1% ($p = 0.011$; $F = 7.2$), 5% ($p = 0.007$; $F = 8.4$), and 10% ($p = 0.02$; $F = 5.9$). In other words, compared with the healthy subjects, the degree of impairment was higher in $FA_{PT}$ than in $FA_{ILF}$ and $FA_{CST}$ in the patients with MTLE at the thresholds 5% and 10% (figure 3A). In contrast, no significant tract-by-group interactions were observed between CST and ILF at any threshold. An example of a significant interaction at the 5% threshold is shown in figure 3B.

3.2.2    Volume of the tracts and MD were also compared between the patients with MTLE and healthy subjects at each threshold. The average MD of the three tracts was higher in the patients. However, we could not detect any significant tract-by-group

interactions at any threshold (figure 4A). As expected, the higher the threshold, the smaller

the volume of each tract became. No tract-by-group interactions were observed at any

threshold (figure 4B).

**3.3 Comparison of white matter integrity using whole brain voxel-wise analysis**

3.3.1    As compared with the healthy control subjects, the whole brain analysis

using TBSS revealed a widespread decreased FA in the MTLE patient group

(Supplementary figure. 1). The decreased FA was not restricted in the

ipsilateral temporal lobe, and distributed in the both hemispheres. The

distribution was wider in the hemisphere ipsilateral to the focus than the

contralateral hemisphere, and involved the ipsilateral putative propagation

tract and the control tracts (ILF, CST).

3.3.2    Increased MD was also observed bilaterally and distributed more

widely on the focus side, including the ipsilateral SPT, ILF, and CST in the

MTLE patients.

**4 Discussion**

4.1    The present combined study of diffusion tractography and FDG-PET led to two

main findings. First, we found massive pathways connecting the epileptic focus and remote

functional deficit zones in the ipsilateral ventrolateral prefrontal area. These pathways

consist mostly of the UF and partly of the AF and the fornix. Second, in MTLE patients,

the integrity of these pathways is more prominently impaired than in the two control

pathways. The extratemporal glucose hypometabolic region identified by us in the

ventrolateral prefrontal cortex ipsilateral to the focus is in good agreement with previous

FDG-PET studies in patients with temporal lobe epilepsy (Arnold et al., 1996; Jokeit et al.,

1997; Takaya et al., 2006). As we expected in our previous study (Takaya et al., 2009),

there is a massive and presumably so exhausted connection through white matter pathways

between the epileptic focus and the prefrontal hypometabolic region. Among them, the UF

is the dominant pathway, suggesting that UF is a major source of influx that is the cause of

the remote functional deficit zone in the prefrontal cortex in patients with MTLE. Two

more pathways, the AF and fornix, were also identified. In the present study, the AF could

be traced because the seed mask was placed in the temporal hypometabolic region that

involves some parts of the middle and superior temporal gyri, which are the cortical

terminals of the long segment of the AF (Martino et al., 2013). The other pathway runs

through the fornix to the thalamus and then to the prefrontal area. This network is probably

related to the hypometabolism and atrophy observed in the ipsilateral thalamus in MTLE

patients (Bonilha et al., 2010; Khan et al., 1997), although group level analysis did not

show significantly decreased glucose uptake in our MTLE group.

4.2 We tested whether a selective or more severe impairment occurs in the PT. For

this purpose, we measured FA, a marker of white-matter integrity, along the given tracts

using tractography-based analysis. In the MTLE patients, all three tracts (PT, ILF, and

CST) showed a significant decrease in FA compared to the control group. This finding is

consistent with previous studies on voxel-wise whole brain analysis using TBSS that

uncovered a widely distributed FA decrease in the white matter networks ipsilateral to the

focus (Focke et al., 2008; Schoene-Bake et al., 2009; Yogarajah et al., 2010). The results

were reproduced in our study (Supplementary figure 1). Furthermore, our study extended

this finding and demonstrated that, in patients with MTLE, FA in the PT ($FA_{PT}$) shows a

much more significant decrease compared with control tracts ($FA_{CST}$ and $FA_{ILF}$),

suggesting that white-matter integrity is more severely impaired in the PT.

4.3 We also measured MD, another indicator of microstructural properties of white

matter. In contrast to FA, the PT in MTLE patients does not show a specific change in MD

compared with the two control tracts. This result may be partly explained by our exclusion

of the most severely affected part of the PT in MTLE patients. In fact, another study

showed that the most significant increase in MD occurs in the regions adjacent to the focus

(Focke et al., 2008), which we excluded from analysis in the present study. In addition,

water diffusivity in these regions varies depending on the time elapsed since the last

seizure (Hufnagel et al., 2003).

4.4        Two possible causes have been proposed as for the change in white-matter

integrity in patients with partial epilepsy in relation to epileptic activity: (1) downstream

degeneration of output fibers (Concha et al., 2012), and (2) propagation of epileptic

activity from the epileptic focus. In our study, the PT is impaired more severely than ILF,

even though both tracts originate in the same region (the anterior part of the

parahippocampal and fusiform gyri (figure 5). If degeneration downstream of the focus is

the main cause of the change in white-matter integrity, the PT and ILF should be damaged

to the same extent. Thus, the propagation of epileptic activity is more likely to cause the

change in white-matter integrity. Moreover, a decrease in $FA_{PT}$ that is not accompanied by

a decrease in volume may further support functional but not degenerative nature of the

impairment. These lines of evidence suggest that the epileptic activity arising from the

focus damages the white matter pathways through which the epileptic activity propagates

to a remote functional deficit zone (Takaya et al., 2009). Another possibility for the change

in white-matter integrity is that inherent pre-existing abnormalities due to genetic factors

or initial precipitating events such as prolonged febrile seizures may also damage the

specific white matter pathways. And because of the impaired white matter integrity, the frequent propagation of epileptic activity may be facilitated. Longitudinal studies are needed to further examine a direct cause-and-effect relationship between epileptic activity and the change in white matter integrity in patients with MTLE.

4.5     There are some limitations in the present study. First, not all patients underwent surgical focus resection, although all of them had clinically and electrophysiologically diagnosed as MTLE. Second, the sample size is not large enough to analyze patients with left and right MTLE separately. We flipped the images from the right-MTLE patients and used images from all patients for the group analysis to increase statistical power. Accordingly, we also flipped images from the same number of healthy subjects for group comparison between the patients and healthy subjects. This approach allowed us to minimize the influence of physiological differences between hemispheres.

4.6     Despite these limitations, our results shed light on the specific network that is associated with functional changes in remote cortical regions during the resting state in patients with MTLE. Further studies are needed that involve diffusion MRI tractography and task-activation fMRI to assess the role of the PT in the functional impairment during cognitive processing in these remote cortical regions.

**5 Conclusions**

5.1 Our results showed that the integrity of white matter pathways that connect the epileptic focus with remote functional deficit regions was specifically impaired. Our findings provide insight into the wide range of functional impairment in patients with localization-related epilepsy.

**Disclosure**

**None of the authors has any conflict of interest to disclose.**

**REFERENCES**

Arnold, S., Schlaug, G., Niemann, H., Ebner, A., Luders, H., Witte, O.W., Seitz, R.J., 1996. Topography of interictal glucose hypometabolism in unilateral mesiotemporal epilepsy. Neurology 46, 1422-1430.

Behrens, T.E., Berg, H.J., Jbabdi, S., Rushworth, M.F., Woolrich, M.W., 2007. Probabilistic diffusion tractography with multiple fibre orientations: What can we gain? Neuroimage 34, 144-155.

Bonilha, L., Elm, J.J., Edwards, J.C., Morgan, P.S., Hicks, C., Lozar, C., Rumboldt, Z., Roberts, D.R., Rorden, C., Eckert, M.A., 2010. How common is brain atrophy in patients with medial temporal lobe epilepsy? Epilepsia 51, 1774-1779.

Catani, M., Jones, D.K., Donato, R., Ffytche, D.H., 2003. Occipito-temporal connections in the human brain. Brain 126, 2093-2107.

Chassoux, F., Semah, F., Bouilleret, V., Landre, E., Devaux, B., Turak, B., Nataf, F., Roux, F.X., 2004. Metabolic changes and electro-clinical patterns in mesio-temporal lobe epilepsy: a correlative study. Brain 127, 164-174.

Concha, L., Kim, H., Bernasconi, A., Bernhardt, B.C., Bernasconi, N., 2012. Spatial patterns of water diffusion along white matter tracts in temporal lobe

epilepsy. Neurology 79, 455-462.

Coste, S., Ryvlin, P., Hermier, M., Ostrowsky, K., Adeleine, P., Froment, J.C., Mauguiere, F., 2002. Temporopolar changes in temporal lobe epilepsy - A quantitative MRI-based study. Neurology 59, 855-861.

Dupont, S., Croize, A.C., Semah, F., Hasboun, D., Samson, Y., Clemenceau, S., Baulac, M., 2001. Is amygdalohippocampectomy really selective in medial temporal lobe epilepsy? A study using positron emission tomography with (18)fluorodeoxyglucose. Epilepsia 42, 731-740.

Focke, N.K., Yogarajah, M., Bonelli, S.B., Bartlett, P.A., Symms, M.R., Duncan, J.S., 2008. Voxel-based diffusion tensor imaging in patients with mesial temporal lobe epilepsy and hippocampal sclerosis. Neuroimage 40, 728-737.

Hufnagel, A., Weber, J., Marks, S., Ludwig, T., De Greiff, A., Leonhardt, G., Widmann, G., Stolke, D., Forsting, M., 2003. Brain diffusion after single seizures. Epilepsia 44, 54-63.

Jokeit, H., Seitz, R.J., Markowitsch, H.J., Neumann, N., Witte, O.W., Ebner, A., 1997. Prefrontal asymmetric interictal glucose hypometabolism and cognitive impairment in patients with temporal lobe epilepsy. Brain 120 ( Pt 12), 2283-2294.

Joo, E.Y., Hong, S.B., Han, H.J., Tae, W.S., Kim, J.H., Han, S.J., Seo, D.W., Lee, K.H., Hong, S.C., Lee, M., Kim, S., Kim, B.T., 2005. Postoperative alteration of cerebral glucose metabolism in mesial temporal lobe epilepsy. Brain 128, 1802-1810.

Khan, N., Leenders, K.L., Hajek, M., Maguire, P., Missimer, J., Wieser, H.G., 1997. Thalamic glucose metabolism in temporal lobe epilepsy measured with 18F-FDG positron emission tomography (PET). Epilepsy Res 28, 233-243.

Love, R., 2005. Two hit hypothesis for temporal lobe epilepsy. Lancet Neurol 4, 458.

Martino, J., De Witt Hamer, P.C., Berger, M.S., Lawton, M.T., Arnold, C.M., de Lucas, E.M., Duffau, H., 2013. Analysis of the subcomponents and cortical terminations of the perisylvian superior longitudinal fasciculus: a fiber dissection and DTI tractography study. Brain Struct Funct 218, 105-121.

Mazziotta, J., Toga, A., Evans, A., Fox, P., Lancaster, J., Zilles, K., Woods, R., Paus, T., Simpson, G., Pike, B., Holmes, C., Collins, L., Thompson, P., MacDonald, D., Iacoboni, M., Schormann, T., Amunts, K., Palomero-Gallagher, N., Geyer, S., Parsons, L., Narr, K., Kabani, N., Le Goualher, G., Boomsma, D., Cannon, T., Kawashima, R., Mazoyer, B., 2001. A probabilistic atlas and

reference system for the human brain: International Consortium for Brain

Mapping (ICBM). Philos Trans R Soc Lond B Biol Sci 356, 1293-1322.

Moran, N.F., Lemieux, L., Kitchen, N.D., Fish, D.R., Shorvon, S.D., 2001.

Extrahippocampal temporal lobe atrophy in temporal lobe epilepsy and mesial

temporal sclerosis. Brain 124, 167-175.

Oguri, T., Sawamoto, N., Tabu, H., Urayama, S., Matsuhashi, M., Matsukawa,

N., Ojika, K., Fukuyama, H., 2013. Overlapping connections within the motor

cortico-basal ganglia circuit: fMRI-tractography analysis. Neuroimage 78,

353-362.

Rosenow, F., Luders, H., 2001. Presurgical evaluation of epilepsy. Brain 124,

1683-1700.

Schoene-Bake, J.C., Faber, J., Trautner, P., Kaaden, S., Tittgemeyer, M., Elger,

C.E., Weber, B., 2009. Widespread affections of large fiber tracts in

postoperative temporal lobe epilepsy. Neuroimage 46, 569-576.

Smith, S.M., Nichols, T.E., 2009. Threshold-free cluster enhancement:

addressing problems of smoothing, threshold dependence and localisation in

cluster inference. Neuroimage 44, 83-98.

Smith, S.M., Kindlemanny, G., Jbabdi, S., 2013. Cross-Subject Comparison of

Local Diffusion MRI Parameters. In Diffusion MRI, Second edition

Song, S.K., Sun, S.W., Ju, W.K., Lin, S.J., Cross, A.H., Neufeld, A.H., 2003. Diffusion tensor imaging detects and differentiates axon and myelin degeneration in mouse optic nerve after retinal ischemia. Neuroimage 20, 1714-1722.

Spanaki, M.V., Kopylev, L., DeCarli, C., Gaillard, W.D., Liow, K., Fazilat, S., Reeves, P., Sato, S., Kufta, C., Theodore, W.H., 2000. Postoperative changes in cerebral metabolism in temporal lobe epilepsy. Arch Neurol 57, 1447-1452.

Takaya, S., Hanakawa, T., Hashikawa, K., Ikeda, A., Sawamoto, N., Nagamine, T., Ishizu, K., Fukuyama, H., 2006. Prefrontal hypofunction in patients with intractable mesial temporal lobe epilepsy. Neurology 67, 1674-1676.

Takaya, S., Mikuni, N., Mitsueda, T., Satow, T., Taki, J., Kinoshita, M., Miyamoto, S., Hashimoto, N., Ikeda, A., Fukuyama, H., 2009. Improved cerebral function in mesial temporal lobe epilepsy after subtemporal amygdalohippocampectomy. Brain 132, 185-194.

Velisek, L., Moshe, S.L., 2003. Temporal lobe epileptogenesis and epilepsy in the developing brain: bridging the gap between the laboratory and the clinic. Progression, but in what direction? Epilepsia 44 Suppl 12, 51-59.

Wakana, S., Caprihan, A., Panzenboeck, M.M., Fallon, J.H., Perry, M., Gollub, R.L., Hua, K., Zhang, J., Jiang, H., Dubey, P., Blitz, A., van Zijl, P., Mori, S., 2007. Reproducibility of quantitative tractography methods applied to cerebral white matter. Neuroimage 36, 630-644.

Yamao, Y., Matsumoto, R., Kunieda, T., Arakawa, Y., Kobayashi, K., Usami, K., Shibata, S., Kikuchi, T., Sawamoto, N., Mikuni, N., Ikeda, A., Fukuyama, H., Miyamoto, S., 2014. Intraoperative dorsal language network mapping by using single-pulse electrical stimulation. Hum Brain Mapp. 35, 4345-4361

Yogarajah, M., Focke, N.K., Bonelli, S.B., Thompson, P., Vollmar, C., McEvoy, A.W., Alexander, D.C., Symms, M.R., Koepp, M.J., Duncan, J.S., 2010. The structural plasticity of white matter networks following anterior temporal lobe resection. Brain 133, 2348-2364.

**FIGURE LEGENDS**

**Figure 1**

**Group comparison between patients and healthy subjects with FDG-PET and the masks in Tractography**

**A.** A group comparison between patients with mesial temporal lobe epilepsy (MTLE) and healthy subjects. A pronounced hypometabolic region, or a functional deficit zone, was observed both in the temporal and frontal areas ipsilateral to the epileptic focus in the MTLE group. The functional deficit zone was observed not only in the mesial temporal area that involved both the hippocampus and parahippocampus but also in the anterior part of the basal and lateral temporal areas. An extratemporal functional deficit zone was recognized in the ipsilateral ventrolateral prefrontal area. **B.** The seed and target masks for tracing the putative propagation tract using tractography. Temporal (blue) and extratemporal (green) hypometabolic areas in the Montreal Neurological Institute (MNI) space (left image) were transferred to the individual T1 anatomical space (middle image), and then segmented for the seed and target masks, respectively (right image). Exclusion masks (white) were placed on the midline sagittal plane and the boundary between the two hypometabolic subregions.

**Figure 2**

**The Propagation tract at each threshold and the control tracts**

The propagation tract (PT) was traced using probabilistic diffusion tractography. PTs

traced at the thresholds 0.1%, 1%, 5%, 10%, and 20% of the maximum connectivity value

are shown (**A**). When the threshold was ≥5%, the uncinate fasciculus (UF) and the arcuate

fasciculus (AF) became predominant, and only the UF remained significant at the 20%

threshold. Control tracts identified at the threshold 5% are shown in panel **B** [corticospinal

tract (CST)] and **C** [inferior longitudinal fasciculus (ILF)].

**Figure 3**

**FA values of CST, ILF, and PT in the MTLE and healthy control groups**

**A.** Mean and standard deviation (SD) of $FA_{CST}$, $FA_{ILF}$, and $FA_{PT}$ are plotted for five

threshold values in the MTLE group (solid line) and the healthy control group (dotted line).

Black circles, white squares, and gray triangles denote mean $FA_{CST}$, $FA_{ILF}$, and $FA_{PT}$,

respectively. **B.** Mean and SD of $FA_{CST}$, $FA_{ILF}$, and $FA_{PT}$ for the MTLE and control groups

at the 5% threshold. As shown in the tracts traced at this representative threshold, there are

significant tract-by-group interactions in the two pairwise analyses: one between ILF and

PT (+; $p = 0.009$) and the other between CST and PT (++; $p = 0.007$), but there is no

interaction between CST and ILF. $FA_{PT}$ decreased more strongly than $FA_{ILF}$ and $FA_{CST}$ did

in the MTLE patients compared with the healthy subjects. The thresholds with significant

tract-by-group interactions in the two pairwise analyses are marked with asterisks in figure

5A (5% and 10%). The experimental conditions are the same as in figure 2.

**Figure 4**

**No significant tract-by-group interactions in mean diffusivity and volume**

**A.** Mean diffusivity (MD) of the seizure propagation tract (PT), corticospinal tract (CST),

and longitudinal fasciculus (ILF) in the mesial temporal lobe epilepsy (MTLE) group and

the control group. No significant tract-by-group interactions were observed at any

threshold. **B.** Volume of PT, ILF, and CST in the MTLE and control group. As the

threshold increased, the volume decreased. No significant tract-by-group interactions were

observed for the tracts traced at any threshold. The experimental conditions are the same as

in figure 3.

**Figure 5**

Tracts displayed near the seed mask in representative patients and healthy subjects. A

putative seizure propagation tract (PT, red), inferior longitudinal fasciculus (ILF, blue), and

corticospinal tract (CST, green) are shown in the axial image at the midbrain level, with the

threshold 5% of the maximum connectivity value. Panel A shows the tracts in six

representative patients with left and right MTLE (upper and lower subpanels, respectively).

Panel B shows the tracts in six representative healthy controls whose tracts were traced in

the left and right hemispheres (upper and lower subpanels, respectively). The seed mask

encompassed the gray matter of the whole temporal hypometabolic region for both PT and

ILF, but the actual seed areas of PT, namely, uncinate fasciculus (UF) and ILF, generally

overlapped in the anterior part of the parahippocampal and fusiform gyri.


Supplementary figure

The whole brain voxelwise statistical analysis of fractional anisotropy (FA) and mean

diffusivity (MD) by using Tract Based Spatial Statistics (TBSS). The MTLE patients are

compared with the healthy control subjects. The hemisphere ipsilateral to the focus is

shown on the left side. In TBSS analysis, the major fasciculi are shown as the mean FA

skeleton (green) in the MNI standard space.

A. Parts of the skeleton colored in red correspond to those of significant FA decrease ($p <$

0.01, corrected for family-wise error rate). Decreased FA in the MTLE group is not

restricted in the ipsilateral temporal lobe where the epileptic focus is located; Decreased

FA is distributed more widely in the hemisphere ipsilateral to the focus than the

contralateral hemisphere, and involves both the ipsilateral seizure propagation tract (PT)

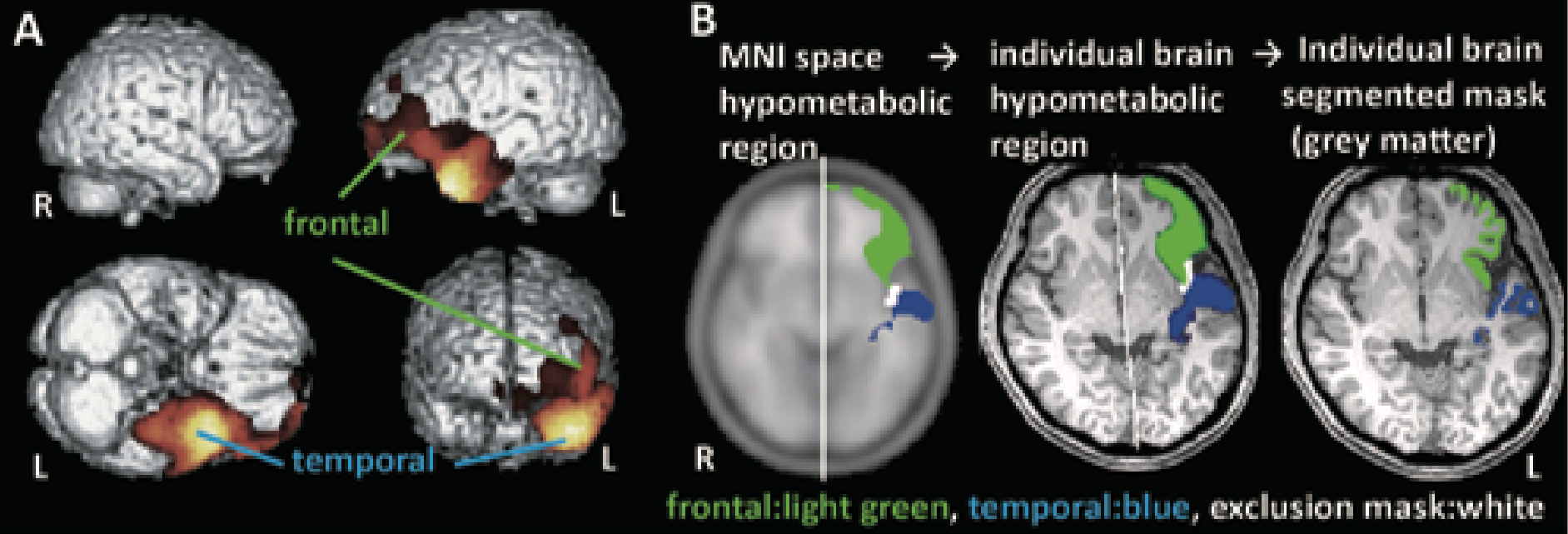and the control tracts (ILF, CST).

Table 1

| Pt.No. | focus | age | onset age | FS | MRI | Seizure semiology | ictal EEG | spike | ope |
|--------|-------|-----|-----------|-----|------|-------------------|-----------|-------|-----|
| 1 | L | 32 | 22 | - | HS, HA | nausea → CPS with dystonic posture of right hand | L | L 80% | - |
| 2 | L | 23 | 19 | - | HS | epigastric rising sensation, ecstacy aura → CPS | L | L | - |
| 3 | L | 45 | 1 | + | HA | epigastric rising sensation → CPS with automatism | not captured | L 98% | - |
| 4 | L | 26 | 12 | - | HS, HA | nausea, psychic aura → CPS | L | L | - |
| 5 | L | 30 | 22 | + | HS, HA | epigastric rising sensation, deja vu and anxious feeling → CPS with automatism | L | L | + |
| 6 | L | 35 | 17 | + | HS | CPS with oral automatism | L | L | - |
| 7 | L | 23 | 22 | + | HS | epigastric rising sensation → CPS | L | - | - |
| 8 | L | 35 | 20 | + | HA | abdominal pain → CPS with oral automatism | no VEEG | L 95% | - |
| 9 | L | 43 | 15 | + | HA | CPS with automatism, and dystonic posture of right hand | L | L | + |
| 10 | L | 43 | 19 | - | HA,HS | CPS with automatism, and dystonic posture of right hand | no VEEG | L | - |
| 11 | R | 38 | 9 | + | HS, HA | nausea → CPS with dystonic posture of left hand | R | R | + |

| | | | | | | | | | |
|---|---|---|---|---|---|---|---|---|---|
| 12 | R | 45 | 5 | + | HS, HA | epigastric rising sensation, psychic aura → CPS | R | R | + |
| 13 | R | 18 | 12 | + | HS, HA | epigastric rising sensation → CPS with automatism and dystonic posture of left hand | R | R | + |
| 14 | R | 23 | 15 | + | HS | CPS with automatism | no VEEG | R | - |
| 15 | R | 25 | 24 | + | HS, HA | nausea → CPS | R | R | - |
| 16 | R | 24 | 12 | - | HS, HA | CPS with automatism | R | R | + |
| 17 | R | 26 | 4 | - | HS, HA | epigastric rising sensation → CPS with automatism | R | R 90% | + |
| 18 | R | 19 | 11 | + | HA | nauseous and uncomfortable feeling → CPS | R | R | + |

FC=febrile convulsion, HS=hippocampal sclerosis, HA=hippocampal atrophy, CPS=complex partial seizure, VEEG=video electroencephalography monitoring

**Figure 1**

A

R, L

frontal

temporal

L, L

B

MNI space hypometabolic region → individual brain hypometabolic region → Individual brain segmented mask (grey matter)

R, L

frontal:light green, temporal:blue, exclusion mask:white

Figure 2

A propagation tract (PT)
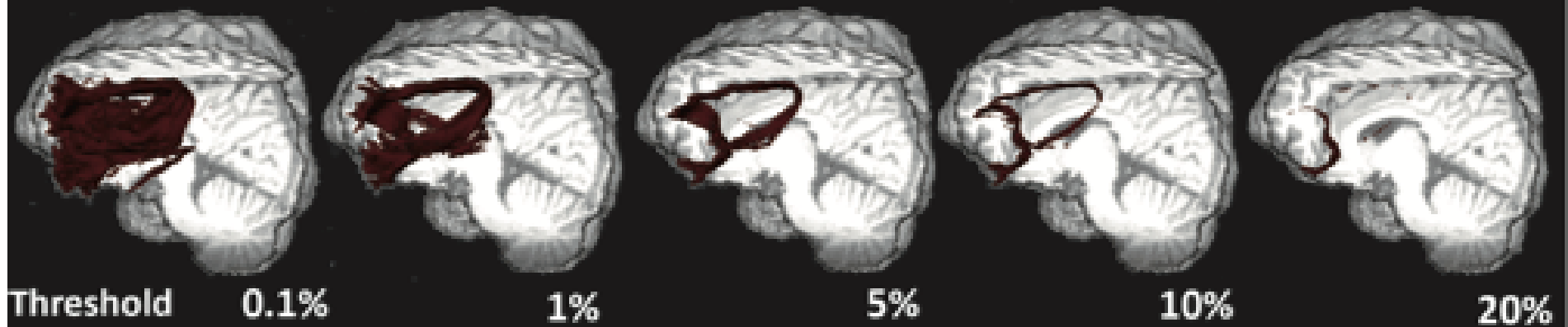
Threshold   0.1%   1%   5%   10%   20%

B cortico-spinal tract (CST)
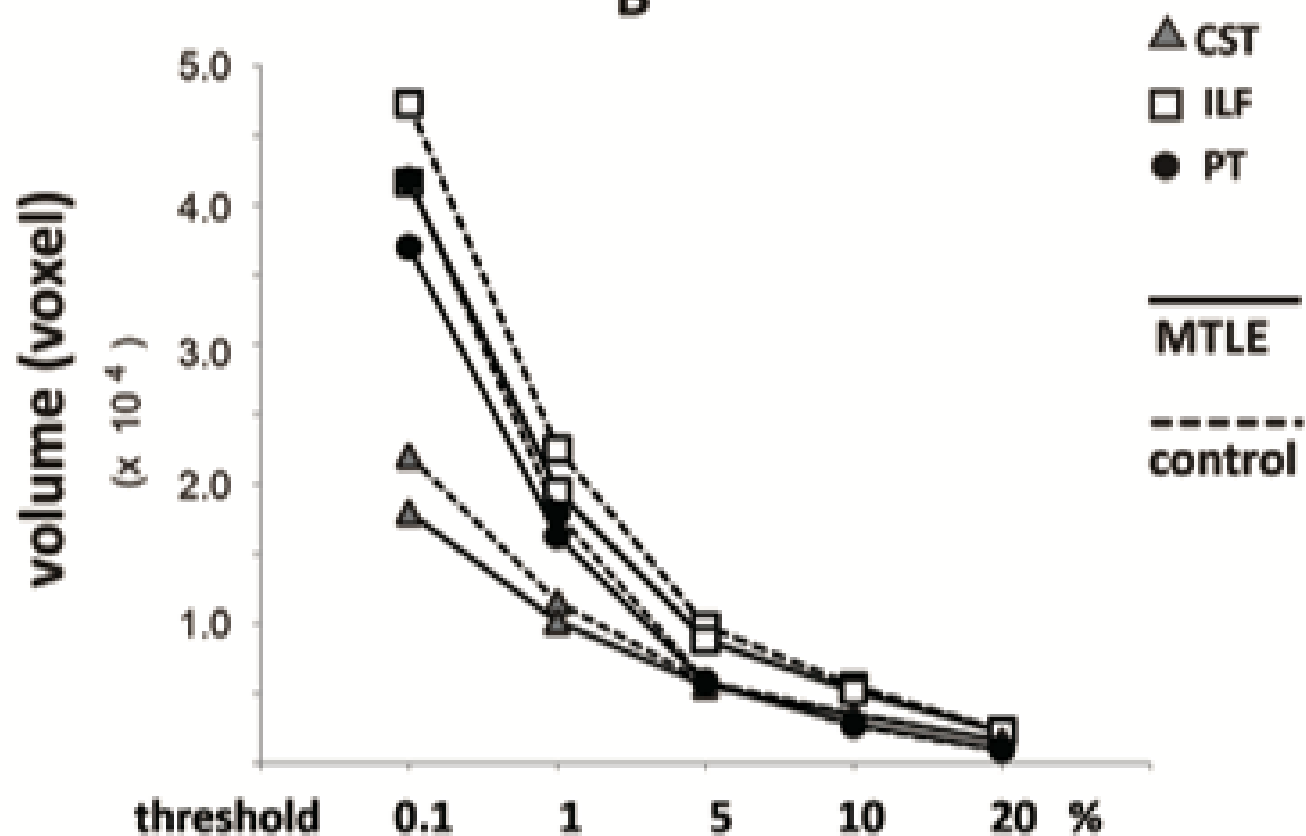
5%

C inferior longitudinal fasciculus (ILF)

5%
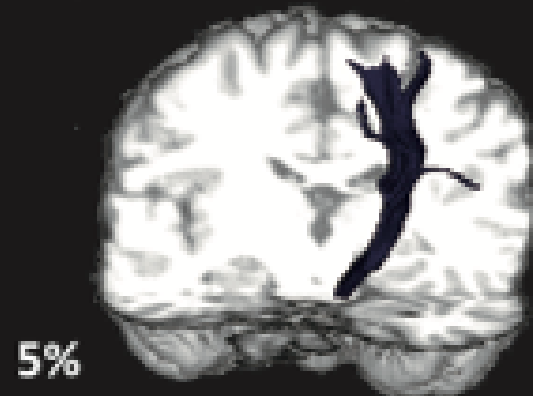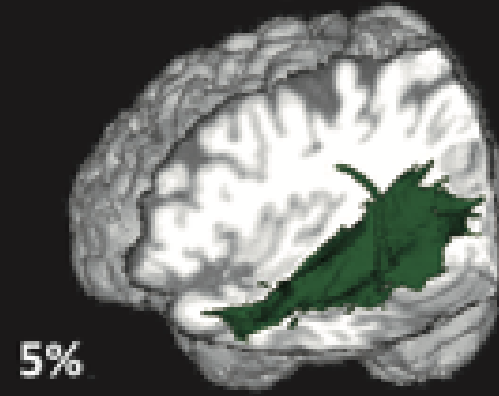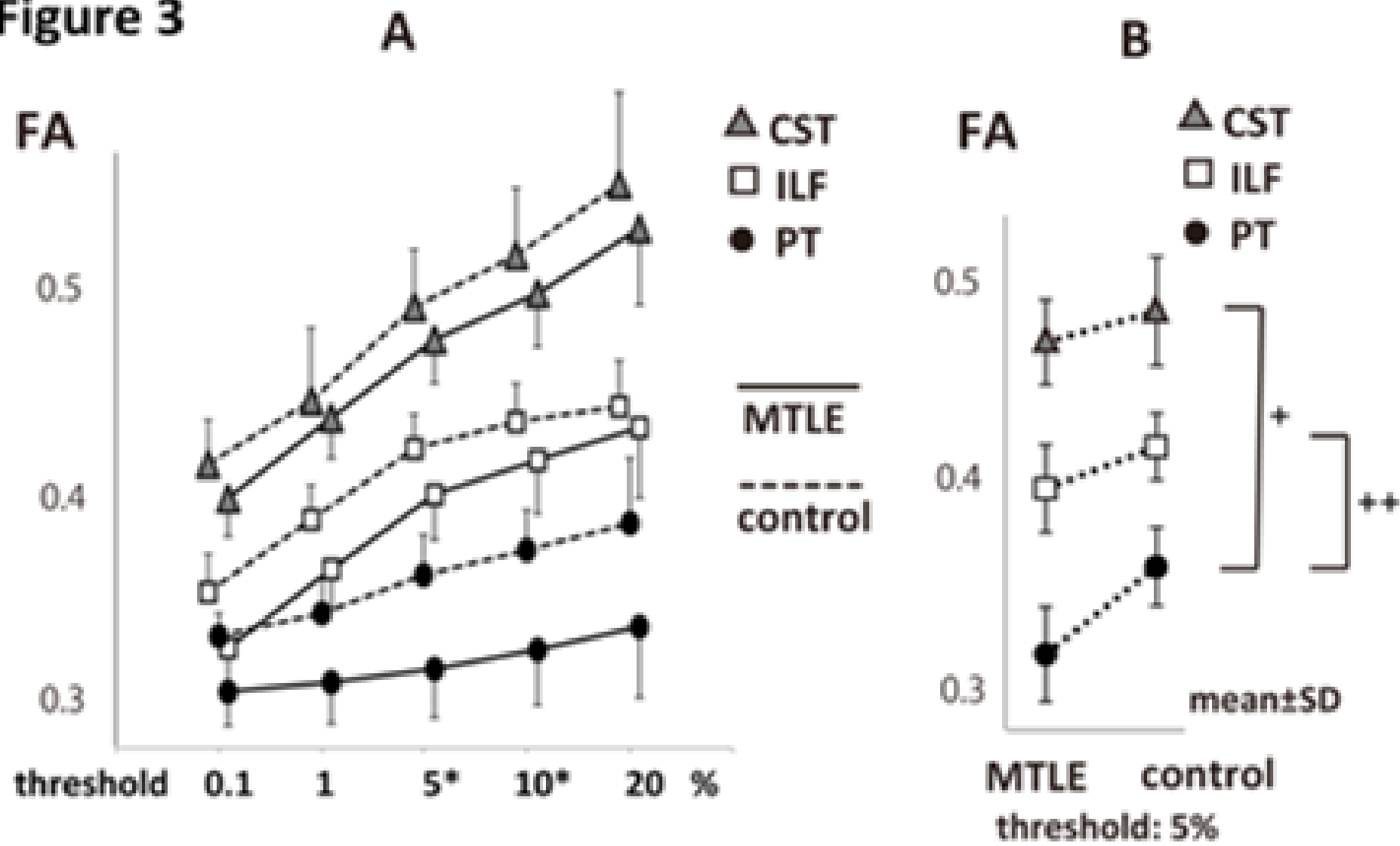
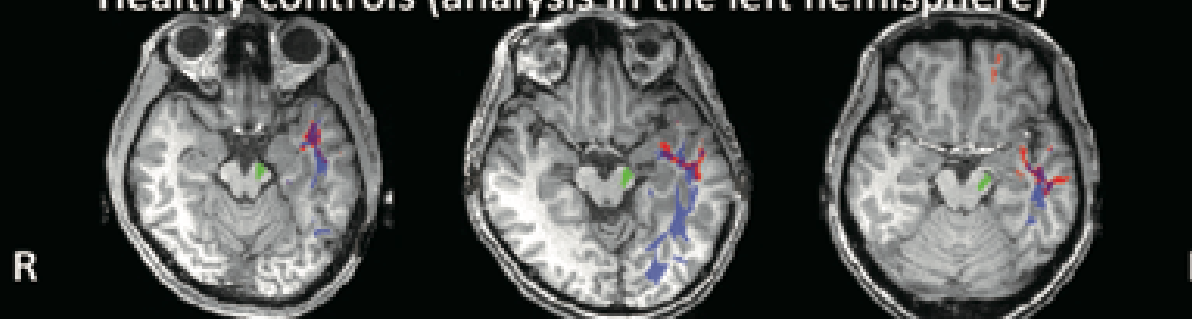# Figure 3

Figure 4
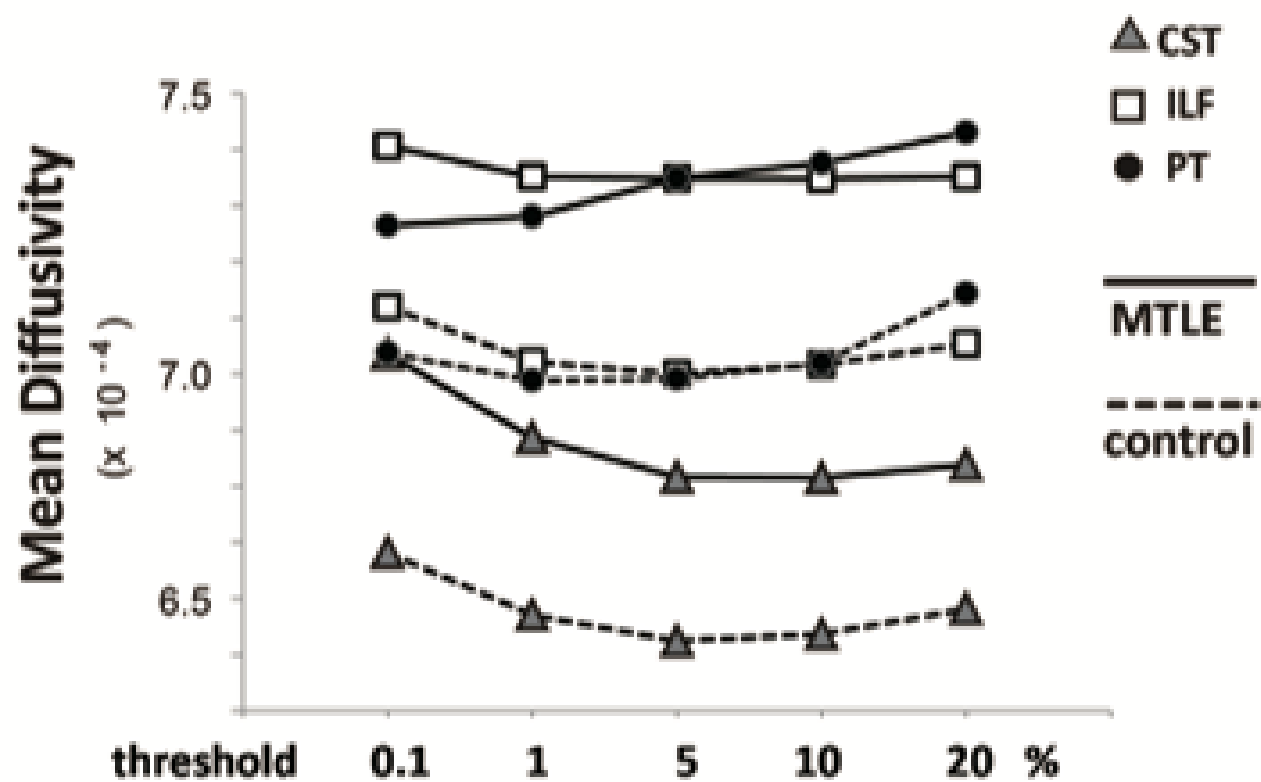
Tracts near the seed mask at the midbrain level
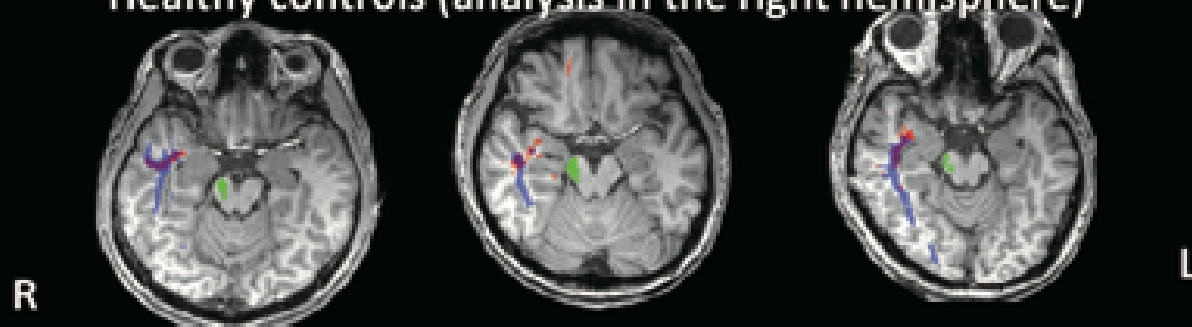
A

Left MTLE

R

L

Right MTLE

R

L
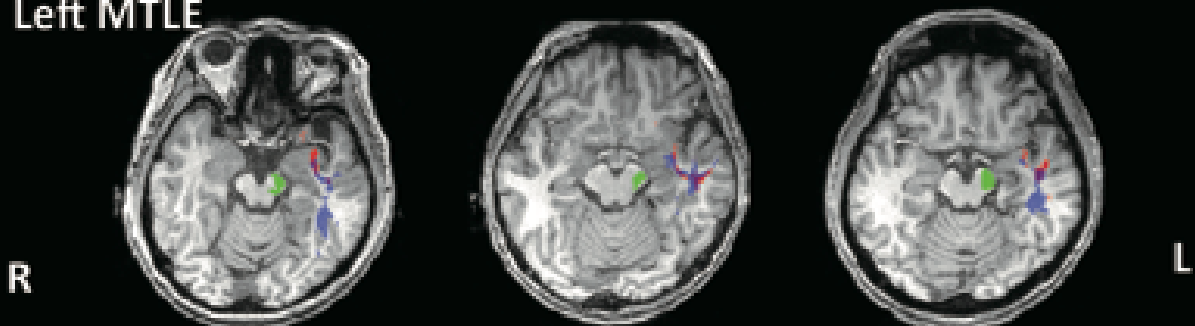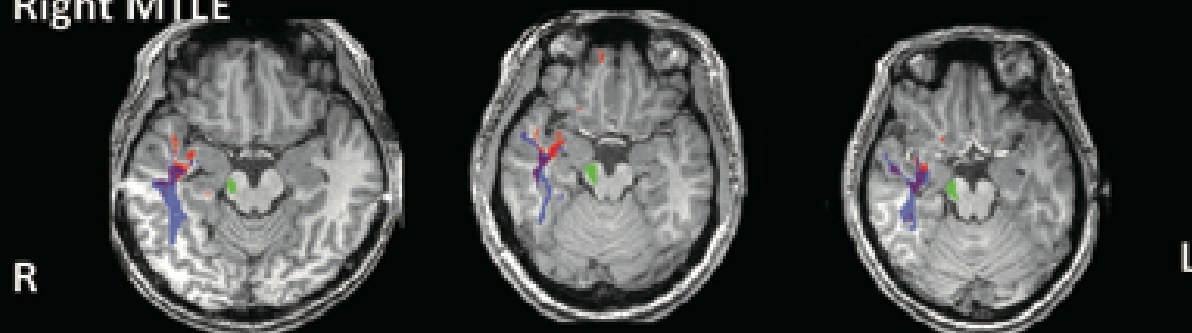
B Healthy controls (analysis in the left hemisphere)

R
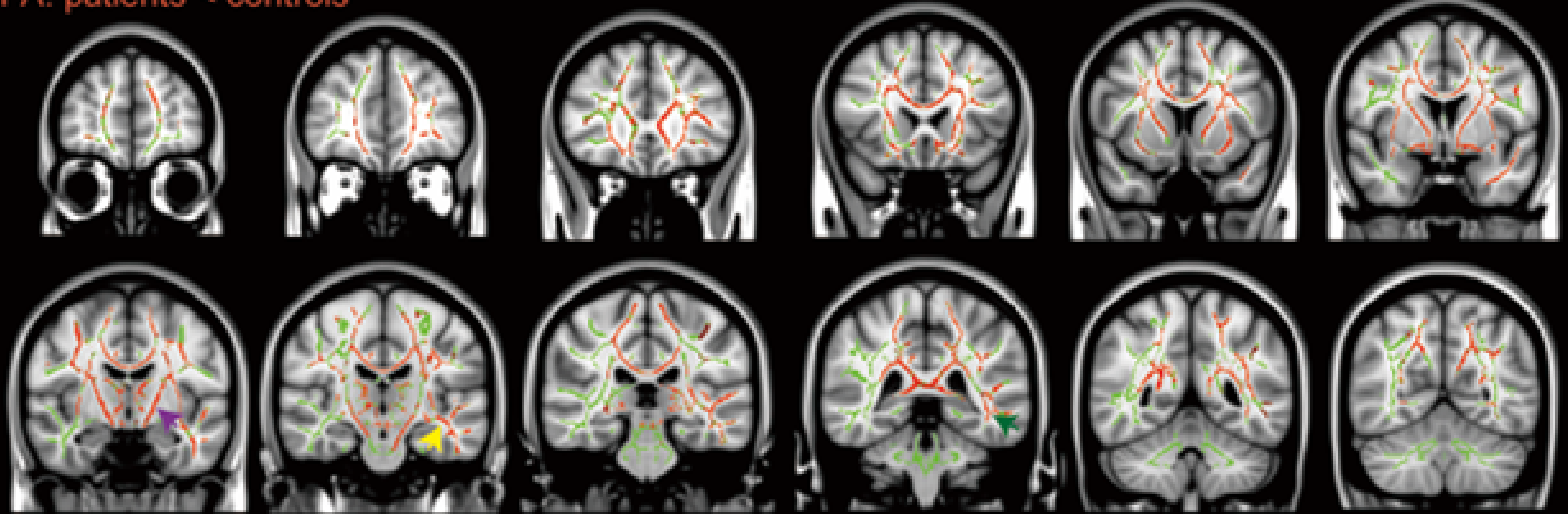
L

Healthy controls (analysis in the right hemisphere)

R
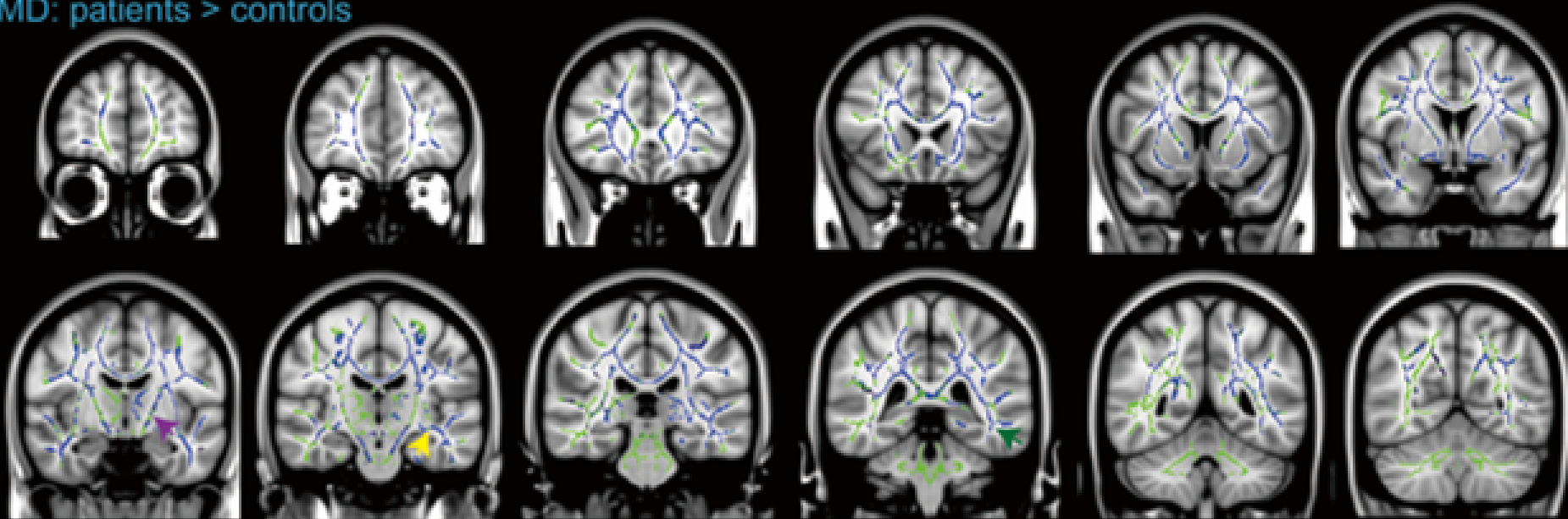
L

PT:red   ILF:blue   CST:green

FA: patients < controls

focus side →

MD: patients > controls

▼ Cortico-spinal tract    ▼ Uncinate fasciculus    ▼ Inferior longitudinal fasciculus